

# The RNA binding protein QKI5 suppresses ovarian cancer via downregulating transcriptional coactivator TAZ

Tao Liu,<sup>1,7</sup> Yu Yang,<sup>1,7</sup> Zhe Xie,<sup>2,7</sup> Qingya Luo,<sup>3</sup> Dan Yang,<sup>1</sup> Xiaoyi Liu,<sup>1</sup> Hongyan Zhao,<sup>1,4</sup> Qinglv Wei,<sup>1</sup> Yi Liu,<sup>1</sup> Lanfang Li,<sup>2</sup> Yuya Wang,<sup>1</sup> Fang Wang,<sup>5</sup> Jianhua Yu,<sup>6</sup> Jing Xu,<sup>1</sup> Jia Yu,<sup>5</sup> and Ping Yi<sup>1</sup>

<sup>1</sup>Department of Obstetrics and Gynecology, The Third Affiliated Hospital of Chongqing Medical University, Chongqing 401120, China; <sup>2</sup>Department of Obstetrics and Gynecology, Research Institute of Surgery, Daping Hospital, Army Medical University, Chongqing 400042, China; <sup>3</sup>Department of Pathology, The First Affiliated Hospital of Army Medical University, Chongqing 400038, China; <sup>4</sup>School of Basic Medical Sciences, Hubei University of Medicine, Shiyuan 442000, China; <sup>5</sup>Department of Biochemistry, Institute of Basic Medical Sciences, Chinese Academy of Medical Sciences (CAMS) & Peking Union Medical College (PUMC), Beijing 100005, China; <sup>6</sup>Department of Hematology and Hematopoietic Cell Transplantation, City of Hope National Medical Center, Duarte, CA 91010, USA

**RNA-binding proteins (RBPs) are a set of proteins involved in many steps of post-transcriptional regulation to maintain cellular homeostasis. Ovarian cancer (OC) is the most deadly gynecological cancer, but the roles of RBPs in OC are not fully understood. Here, we reported that the RBP QKI5 was significantly negatively correlated with aggressive tumor stage and worse prognosis in serous OC patients. QKI5 could suppress the growth and metastasis of OC cells both *in vitro* and *in vivo*. Transcriptome analysis showed that QKI5 negatively regulated the expression of the transcriptional coactivator TAZ and its downstream targets (e.g., CTGF and CYR61). Mechanistically, QKI5 bound to TAZ mRNA and recruited EDC4, thus decreasing the stability of TAZ mRNA. Functionally, TAZ was involved in the QKI5-mediated tumor suppression of OC cells, and QKI5 expression was inversely correlated with TAZ, CTGF, and CYR61 expression in OC patients. Together, our study indicates that QKI5 plays a tumor-suppressive role and negatively regulates TAZ expression in OC.**

## INTRODUCTION

Ovarian cancer (OC) is the most deadly tumor among all gynecological cancers. Around 21,750 new OC cases and 13,940 OC-related deaths have been estimated in the United States in 2020.<sup>1</sup> More than half of the OC patients are diagnosed at advanced stages, with a poor prognosis and a high relapse rate.<sup>2</sup> The 5-year overall survival for women diagnosed at the advanced OC stage is approximately 30%.<sup>1,3</sup> Although various key molecular pathways or OC-related genes have been reported, the mechanisms underlying the pathogenesis of OC remain largely unexplored.<sup>4-6</sup> Thus, unraveling the molecular mechanisms to identify biomarkers or therapeutic targets is of great significance for OC treatment.

RNA-binding proteins (RBPs) participate in almost every aspect of post-transcriptional regulation to maintain cellular homeostasis.

Through regulating RNA splicing, turnover, and translation, RBPs can direct the cell fate and mediate the functions of their target genes. Currently, the relationship between RBPs and disease occurrence has been studied.<sup>7,8</sup> For example, dysfunction of RBPs was found to be associated with neuromuscular and neurological diseases.<sup>9</sup> Moreover, a previous study depicted the expression profiles of more than 1,500 human RBPs in different cancers in The Cancer Genome Atlas (TCGA) database and demonstrated that a number of RBPs were involved in cancer progression.<sup>10</sup> As a RBP, QKI5 had been implicated in the processing of microRNA (miRNA) and pre-mRNA and was downregulated in several cancers.<sup>11-14</sup> However, the exact roles and detailed mechanisms of QKI5 in OC are still ambiguous.

In this research, we demonstrated that QKI5 was markedly downregulated in serous OC (SOC) and the low level of QKI5 expression predated a poor prognosis. We also reported that QKI5 could inhibit the growth and metastasis of OC cells both *in vivo* and *in vitro*. Mechanistically, transcriptional coactivator with PDZ binding motif (TAZ) was identified as the key target of QKI5 by transcriptome analysis. QKI5 negatively regulated the expression of TAZ by interacting with its mRNA and decreasing its stability. This study describes a novel QKI5-TAZ regulatory mechanism in OC, and QKI5 can serve as a potential biomarker for OC management.

Received 17 May 2021; accepted 17 July 2021;  
<https://doi.org/10.1016/j.omtn.2021.07.012>

<sup>7</sup>These authors contributed equally

**Correspondence:** Jia Yu, Department of Biochemistry, Institute of Basic Medical Sciences, Chinese Academy of Medical Sciences (CAMS) & Peking Union Medical College (PUMC), Beijing 100005, China.  
**E-mail:** [j-yu@ibms.pumc.edu.cn](mailto:j-yu@ibms.pumc.edu.cn)

**Correspondence:** Ping Yi, Department of Obstetrics and Gynecology, The Third Affiliated Hospital of Chongqing Medical University, Chongqing 401120, China.  
**E-mail:** [yiping@cqmu.edu.cn](mailto:yiping@cqmu.edu.cn)



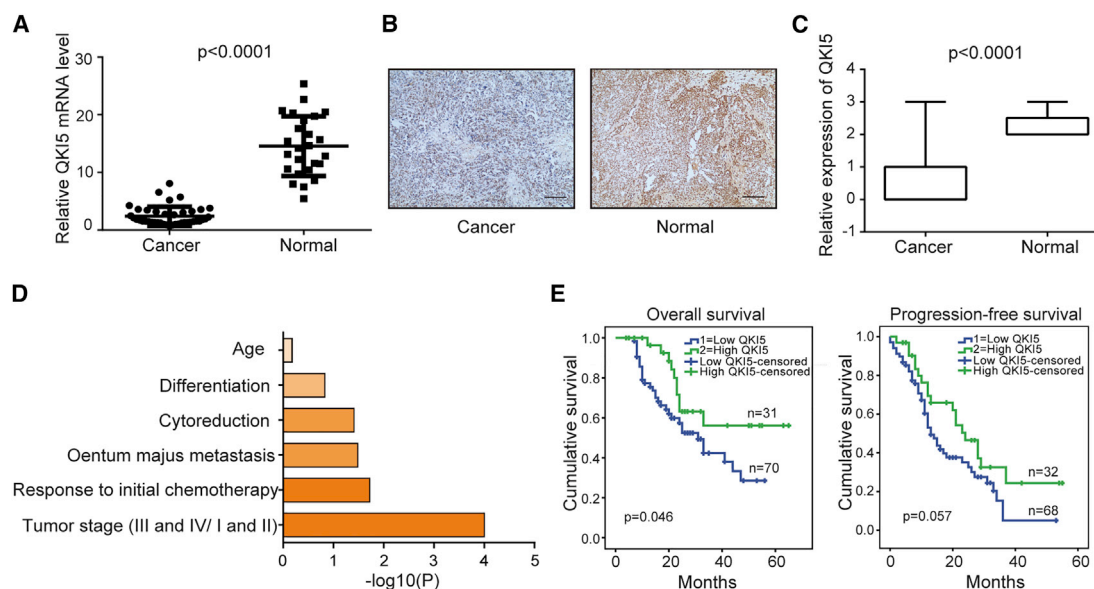


**Figure 1. Low expression level of QKI5 is associated with tumorigenesis and poor outcome of OC patients**

(A) Transcript levels of QKI5 were determined by qRT-PCR in fresh frozen tumor specimens ( $n = 40$ ) and hNOSE samples ( $n = 27$ ). The reference gene was GAPDH. (B) Representative immunohistochemistry pictures of QKI5 protein expression level in primary tumor tissues and normal ovarian epithelial tissues. Original magnification,  $\times 100$ . Scale bar,  $100 \mu\text{m}$ . (C) Relative QKI5 protein expression was assessed by tissue microarray analysis in FFPE OC specimens ( $n = 134$ ) and normal FFPE ovarian surface epithelial tissues ( $n = 40$ ).  $p < 0.0001$ . (D) Association analysis of QKI5 protein expression with clinicopathological features.  $p$  values were calculated by using the chi-square test. (E) Progression-free survival and overall survival curves of OC patients with low or high QKI5 expression. According to the median QKI5 immunohistochemical stain score, patients were divided into two subgroups. Log-rank test was employed for the comparative analysis.

## RESULTS

### Downregulation of QKI5 expression contributes to SOC progression and poor prognosis

To identify the functional role of QKI5 in OC, we detected and compared the levels of QKI5 in SOC tissues and human normal ovarian surface epithelium (hNOSE). First, we examined the RNA level of QKI5 in 40 SOC specimens and 27 hNOSE samples by qRT-PCR and found that QKI5 was markedly downregulated in SOC tissues (Figure 1A). In line with this, the results from tissue microarray involving 134 SOC specimens and 40 hNOSE samples demonstrated that the protein level of QKI5 was downregulated in OC tissues (Figures 1B and 1C; Figure S1). To explore the relationships between QKI5 expression and clinicopathologic characteristics, we used both univariate and multivariable logistic regression tests. The clinicopathological features of OC patients were reported in our previous study.<sup>15</sup> The findings revealed that QKI5 downregulation was correlated with aggressive tumor stage, omentum majus metastasis, cytoreduction, and sensitivity to initial chemotherapy. However, as shown in Table 1 and Figure 1D, no significant correlation of QKI5 expression with age or differentiation was found. Apart from QKI5 downregulation, aggressive tumor stage, omentum majus metastasis, cytoreduction, and sensitivity to initial chemotherapy were also correlated with overall survival, as indicated by univariate analysis (Table 1). The survival curve reflected that OC patients with higher QKI5 protein level had a longer overall survival but exhibited no significant difference in progression-free survival

(Figure 1E; Tables S1 and S2). These results demonstrate a potential role of QKI5 in SOC progression.

### QKI5 suppresses OC cell growth and induces apoptosis

Then gain- and loss-of-function experiments were performed in OC cells to elucidate the biological functions of QKI5 in this disease. QKI5 was alternatively overexpressed or knocked down in A2780 and SKOV3 cell lines (Figure 2A). The results of cell counting kit-8 (CCK-8) assays showed that QKI5 overexpression inhibited the proliferation of OC cells: and conversely, QKI5 knockdown increased OC cell proliferation (Figure 2B). To further determine the cytotoxic effect of QKI5 on OC cells, we conducted flow cytometric analysis to examine cell-cycle distribution and apoptotic death. Ectopic QKI5 expression increased the accumulation of OC cells in the G1 phase, together with a low level of S-phase cell population. On the contrary, QKI5 depletion reduced the amount of OC cells in the G1 phase, along with a high level of S-phase cell population (Figures 2C and 2D). Besides, we also found that the apoptotic rate of OC cells was increased upon QKI5 overexpression, while QKI5 knockdown suppressed the apoptosis of OC cells (Figures 2E and 2F). These data imply that QKI5 suppresses the proliferation and induces the apoptosis of OC cells.

### QKI5 suppresses the tumorigenicity of OC cells in mice

To determine the effect of QKI5 expression on OC cell tumorigenesis *in vivo*, we injected the QKI5-overexpressed (pCMV6-QKI5) or

**Table 1. Associations of QKI5 expression with clinicopathologic characteristics of ovarian cancer**

Characteristics	QKI5 expression		X2	p value
	High (n, %)	Low (n, %)		
Age - year			0.175	0.676
>50	6 (4.5%)	75 (56.0%)		
≤50	5 (3.7%)	48 (35.8%)		
Tumor stage - no. (%)			16.713	0.000
I or II	10 (7.5%)	28 (20.9%)		
III or IV	2 (1.5%)	94 (70.1%)		
Differentiation - no. (%) well	2 (6.7%)	7 (23.3%)	2.083	0.149
Poorly	10 (33.3%)	115 (36.7%)		
Omentum majus metastasis - no. (%)			4.527	0.033
Absent	8 (5.9%)	39 (28.9%)		
Present	5 (3.7%)	83 (61.5%)		
Cytoreduction - no. (%)*			4.266	0.039
Optimal	10 (7.5%)	73 (54.5%)		
Suboptimal	1 (0.7%)	50 (37.3%)		
Response to initial chemotherapy - no. (%)			5.466	0.019
Sensitive	11 (10.1%)	55 (50.5%)		
Resistant	1 (0.9%)	42 (38.5%)		

p values were calculated after missing values were excluded.

QKI5-silenced (shQKI5-1 and shQKI5-2) A2780 OC cells or control cells (pCMV6 or pSIH) into the nude mice. The tumors grown in mice with QKI5-overexpressed cells were notably smaller than those in the control group. Conversely, the tumors grown in mice with QKI5-silencing cells were larger than those in the control group (Figure 3A). The average tumor weight and volume at sacrifice were lower in mice with QKI5 overexpression and higher in mice with QKI5 knockdown, respectively, compared to their corresponding control mice (Figures 3B and 3C).

Subsequently, we examined the cell proliferative and apoptotic indices in these OC tissues. Immunohistochemistry staining demonstrated that the proportion of Ki67-positive cells in the tumor tissues collected from QKI5 overexpression group was lower compared to the control group, while the QKI5 knockdown group displayed more Ki67-positive cells (Figures 3D–3F). The apoptosis index was analyzed by active caspase-3 staining and was significantly increased in mice bearing tumors with QKI5 overexpression compared to the control mice. On the contrary, QKI5 knockdown led to a decrease in active caspase-3 staining in the mice bearing tumors compared to the control mice (Figures 3D–3F).

### QKI5 regulates OC cell metastasis

Next, Transwell assays were conducted to assess the effects of QKI5 on OC cell migration and invasion abilities. QKI5 overexpression

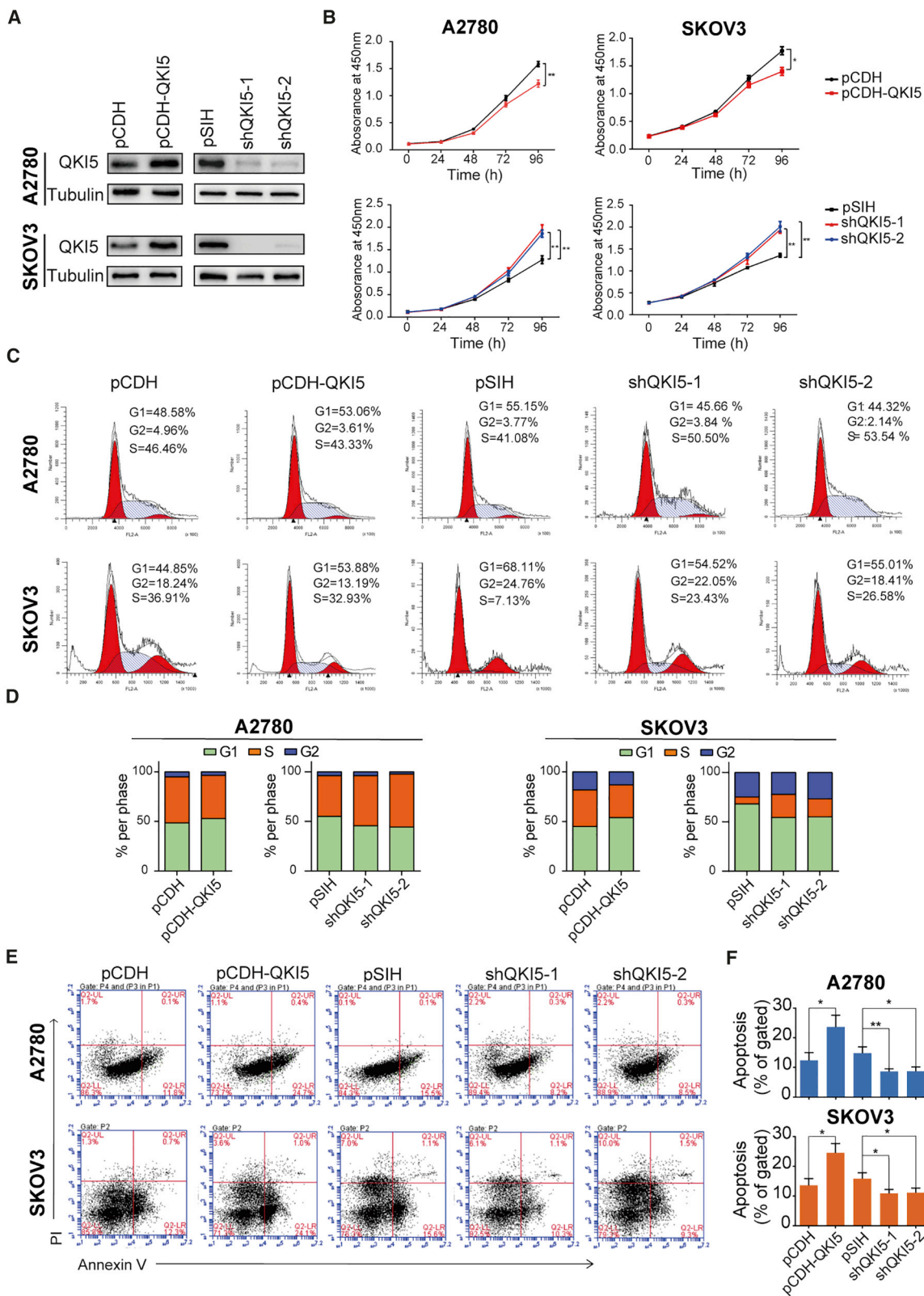
markedly impaired the migration of A2780 and SKOV3 cells, whereas QKI5 silencing promoted the migration of these OC cells (Figures 4A–4D). Similar to the results of cell migration, matrigel invasion assays revealed that ectopic QKI5 expression suppressed the invasion of A2780 and SKOV3 cells; and conversely, QKI5 depletion promoted OC cell invasion compared to the control cells (Figures 4A–4D). These findings reveal that QKI5 negatively regulates the metastasis of OC cells *in vitro*.

Furthermore, we conducted *in vivo* metastasis assays by injecting the QKI5-overexpressed or QKI5-depleted A2780 OC cells or control cells into the lateral tail vein of nude mice. After executing the mice at 10 weeks post-injection, the lungs and livers were isolated. All lung and liver samples did not show any large metastasis nodules in these experimental groups (Figure S2). The lungs and livers were then dissected for histological examination via hematoxylin and eosin staining. The results showed that metastatic foci were found in the lung sections but not in the liver sections of the tumor xenografts (Figure 4E). The number of metastatic foci was markedly decreased in the lung sections of mice with QKI5 overexpressing tumors compared to the control group. Conversely, the lungs of mice with QKI5-depleting tumors possessed more metastatic foci compared to the control group (Figure 4F). Altogether, these data indicate QKI5 impairs the tumorigenicity and metastasis of OC cells *in vivo*.

### QKI5 controls transcript abundance in OC cells

Our results strongly suggest that QKI5 can act as a tumor suppressor gene in OC. As an RNA binding protein, QKI5 is able to regulate RNA fate through post-transcriptional regulation (e.g., alternative splicing and mRNA stability).<sup>16–19</sup> To further identify the targets of QKI5 involved in the regulation of OC cell growth and metastasis at a transcriptome-wide level, we conducted gene expression profiling in A2780 cells after QKI5 knockdown via RNA sequencing (RNA-seq). Notably, QKI5 knockdown altered the abundance of 2,482 genes (fold-change > 1.5 and  $p < 0.05$ ), of which 1,517 genes were downregulated and 965 genes were upregulated (Figure 5A). Gene ontology (GO) analysis of these differentially expressed genes revealed multiple distinct gene clusters such as protein binding, cytoplasm, cytosol, and mitogen-activated protein kinase (MAPK) signaling pathway (Figure 5B).

QKI5 harbors a homology domain of KH protein family and binds with the QKI response element (QRE) sequence (NACUAAYN<sub>1–20</sub>UAAAY).<sup>20</sup> A previous study has identified a set of transcripts with the QRE sequence through a genome-wide computational analysis.<sup>16</sup> Thus, we overlapped the genes with QRE sequences and 2,482 differentially expressed genes in OC cells after QKI5 knockdown and found that 210 genes (including 108 downregulated genes and 102 upregulated genes) were composed of the QRE sequences (Figures 5C and 5D). The top five differentially expressed genes with QRE sequences in A2780 cells after QKI5 knockdown are shown in Figure 5E. These RNA-seq results were then validated by qRT-PCR and the expression levels of selected genes were assessed. Interestingly, a significant consensus was observed between the qRT-PCR and RNA-seq results



(legend on next page)



(Figures 5F and 5G). Hence, these data strongly imply that QKI5 controls the transcript abundance in OC cells.

### QKI5 represses the expression of TAZ by affecting its mRNA stability

Among the 210 differentially expressed genes with QRE sequences, the transcriptional cofactor TAZ was significantly upregulated; and more importantly, the downstream genes of TAZ (e.g., CTGF and CYR61) were also upregulated in both RNA-seq and qRT-PCR results. TAZ, CTGF, and CYR61 are implicated in the Hippo pathway, and imbalance of this pathway has been observed in many types of human cancer. In Hippo pathway, TAZ binds directly to the TEAD family of transcriptional factors and subsequently promotes the transcription of downstream targets (e.g., CTGF and CYR61).<sup>21,22</sup> Importantly, it has been reported that TAZ could promote the proliferation and migration of OC cells.<sup>23</sup> Hence, TAZ was selected as a potential key target of QKI5, and its effect on QKI5-mediated tumor suppression was further investigated.

We first assessed the abundance of TAZ, CTGF, and CYR61 in A2780 and SKOV3 cells after QKI5 knockdown. QKI5 depletion increased the expression of TAZ, CTGF, and CYR61 at both RNA and protein levels (Figures 6A and 6B). Subsequently, RNA immunoprecipitation (RIP) assays were performed in A2780 cells with overexpression of FLAG-tagged QKI5. The qRT-PCR results showed that TAZ mRNA, but not glyceraldehyde-3-phosphate dehydrogenase (GAPDH) mRNA, was enriched using a FLAG-specific antibody after normalization to immunoglobulin G (IgG; Figure 6C). In previous studies,<sup>16,17</sup> QKI5 was reported to regulate the abundance of its targets by affecting the decay of the target mRNAs. Thus, we speculate that QKI5 may negatively regulate TAZ expression through inducing QKI5 mRNA decay. To test this hypothesis, we treated the OC cells with QKI5 knockdown with the transcription inhibitor actinomycin D and performed qRT-PCR to assess the stability of TAZ mRNA. The results demonstrated that the stability of TAZ mRNA was strikingly increased after QKI5 knockdown (Figure 6D). Several factors involved in RNA decay were identified by QKI5 IP and mass spectral analysis (data not shown), among which EDC4 might serve as an enhancer of mRNA turnover.<sup>24</sup> The results of IP assays revealed that QKI5 could interact with EDC4, suggesting that QKI5 may promote RNA decay through recruiting EDC4 (Figure 6E).

### TAZ is involved in the QKI5-mediated tumor suppression of OC cells

To determine whether the influence of QKI5 on OC cells was dependent on TAZ expression, the transcriptional activity of TAZ was silenced in QKI5-depleting OC cells. Immunoblotting analysis revealed that the expressions of TAZ, CTGF, and CYR61 were

upregulated after QKI5 knockdown, and TAZ silencing in QKI5-depleted cells could decrease the expression of CTGF and CYR61 (Figure 7A). Growth curves showed that the QKI5 knockdown-induced proliferation rates of OC cells were partially abrogated after TAZ knockdown (Figure 7B). Besides, the migration and invasion abilities of OC cells were promoted after QKI5 knockdown, while TAZ silencing could suppress OC cell migration and invasion (Figures 7C and 7D). These findings indicate that the QKI5-mediated tumor suppression of OC cells is partially dependent on TAZ activation.

QKI5 negatively regulates the expression of TAZ and its downstream targets CTGF and CYR61 in OC cells. To verify this association in clinical samples, we measured the expression levels of QKI5, TAZ, CTGF, and CYR61 in 41 OC samples and their matched normal ovarian epithelial tissues and analyzed the correlations among QKI5, TAZ, CTGF, and CYR61, respectively. As shown in Figures 7E–7G, the expression of QKI5 was inversely correlated with TAZ expression, as well as CTGF and CYR61 expression. These data indicate that QKI5 reduces the expression of TAZ to exert its suppressive effect on OC patients.

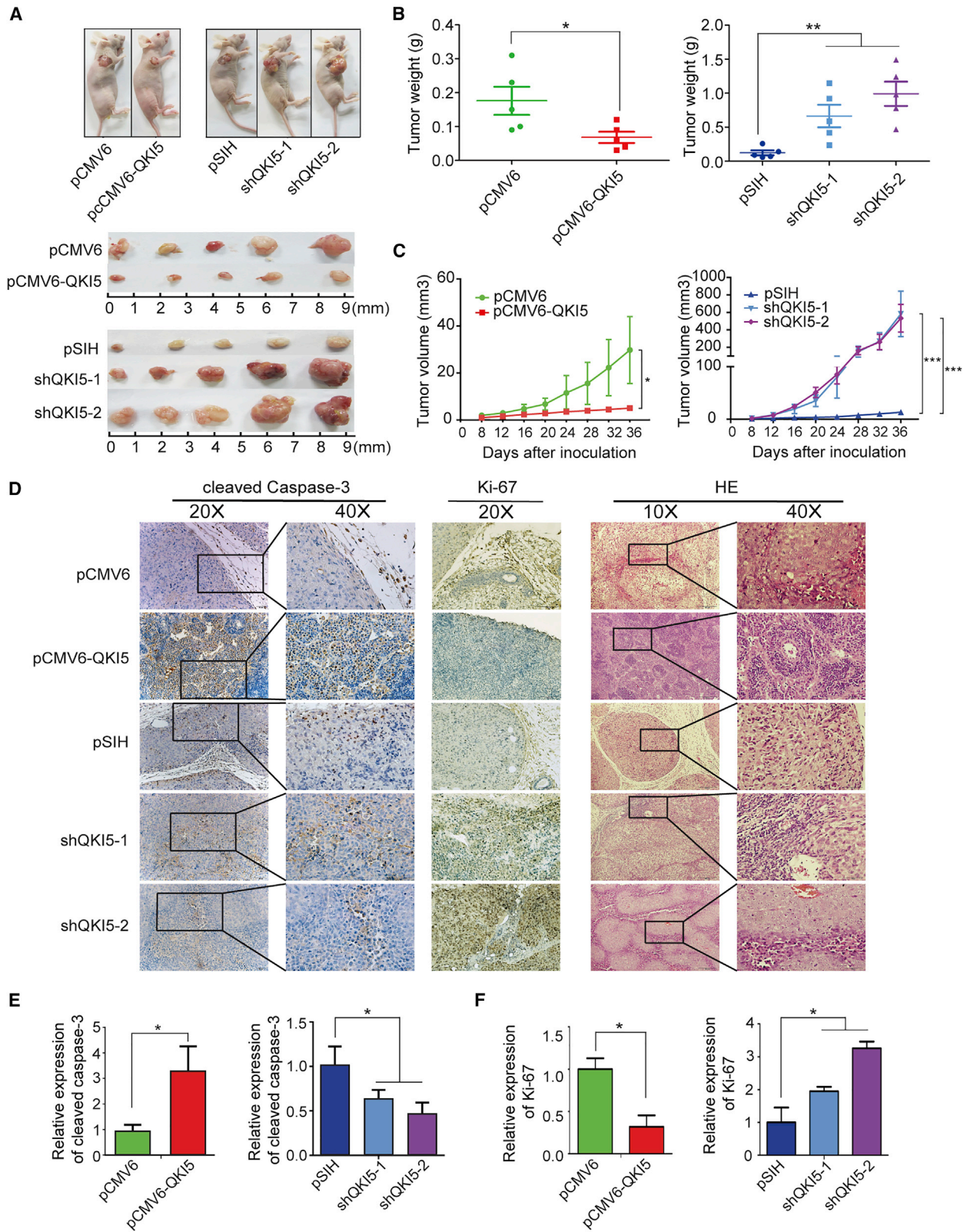
## DISCUSSION

Our study demonstrated that QKI5 exerted tumor suppressive effect on OC. The expression of QKI5 was remarkably decreased in OC tissues and was associated with a worse prognosis. Moreover, QKI5 depletion could promote the tumorigenesis and metastasis of OC cells both *in vitro* and *in vivo*. In addition, we identified the targets of QKI5 in OC cells via transcriptomic analysis. As illustrated in Figure 8, QKI5 could decrease the stability of TAZ mRNA, concomitant with a decline in the protein expression of TAZ and its downstream targets (CTGF and CYR61). These findings suggest that the depletion of QKI5 significantly contributes to OC progression.

QKI5 is an isoform of the RBP QKI, and other isoforms are designated as QKI6 and QKI7. QKI5 is the only nuclear isoform that shuttles between cytoplasm and nucleus, while QKI6 and QKI7 isoforms are located mostly in the cytoplasm.<sup>25,26</sup> In this study, the expression levels of QKI6 and QKI7 in OC tissues were detected and compared with those in ovarian epithelial cells. We found that these two isoforms were downregulated in accordance with the expression pattern of QKI5 in OC cells (Figure S3). QKI isoforms are highly conserved RBPs that belong to the family of STAR (signal transduction and activation of RNA).<sup>19,27</sup> QKI is highly expressed in the lungs, brain, heart, and testis of adults and can be affected by developmental stages.<sup>28,29</sup> In the nervous system, the proteins of QKI are key components in the regulation of oligodendrocyte differentiation and myelination.<sup>30,31</sup> QKI depletion could promote the tumorigenesis of gastric cancer and lung cancer cells.<sup>13,14</sup> A recent cross-linking-immunoprecipitation and high-throughput sequencing (CLIP-

### Figure 2. QKI5 suppresses cell growth and promotes apoptosis in OC cells

(A) Overexpression or knockdown of QKI5 expression in OC cells was established by lentivirus infection. The protein levels of QKI5 in these cells were detected by immunoblotting at 48 h after infection (tubulin was used as the reference gene). (B) Effect of QKI5 overexpression or knockdown on the proliferation of OC cells was analyzed through CCK-8 assays. (C and D) Effect of QKI5 overexpression or knockdown on the cell cycle distribution of OC cells was determined by PI staining and flow cytometry. (E and F) Effect of QKI5 overexpression or knockdown on the apoptosis of OC cells followed by H<sub>2</sub>O<sub>2</sub> treatment was determined by Annexin V/PI staining and flow cytometry. All data were expressed as mean ± SD. \*p < 0.05, \*\*p < 0.01, \*\*\*p < 0.001, according to Student's t test.



(legend on next page)



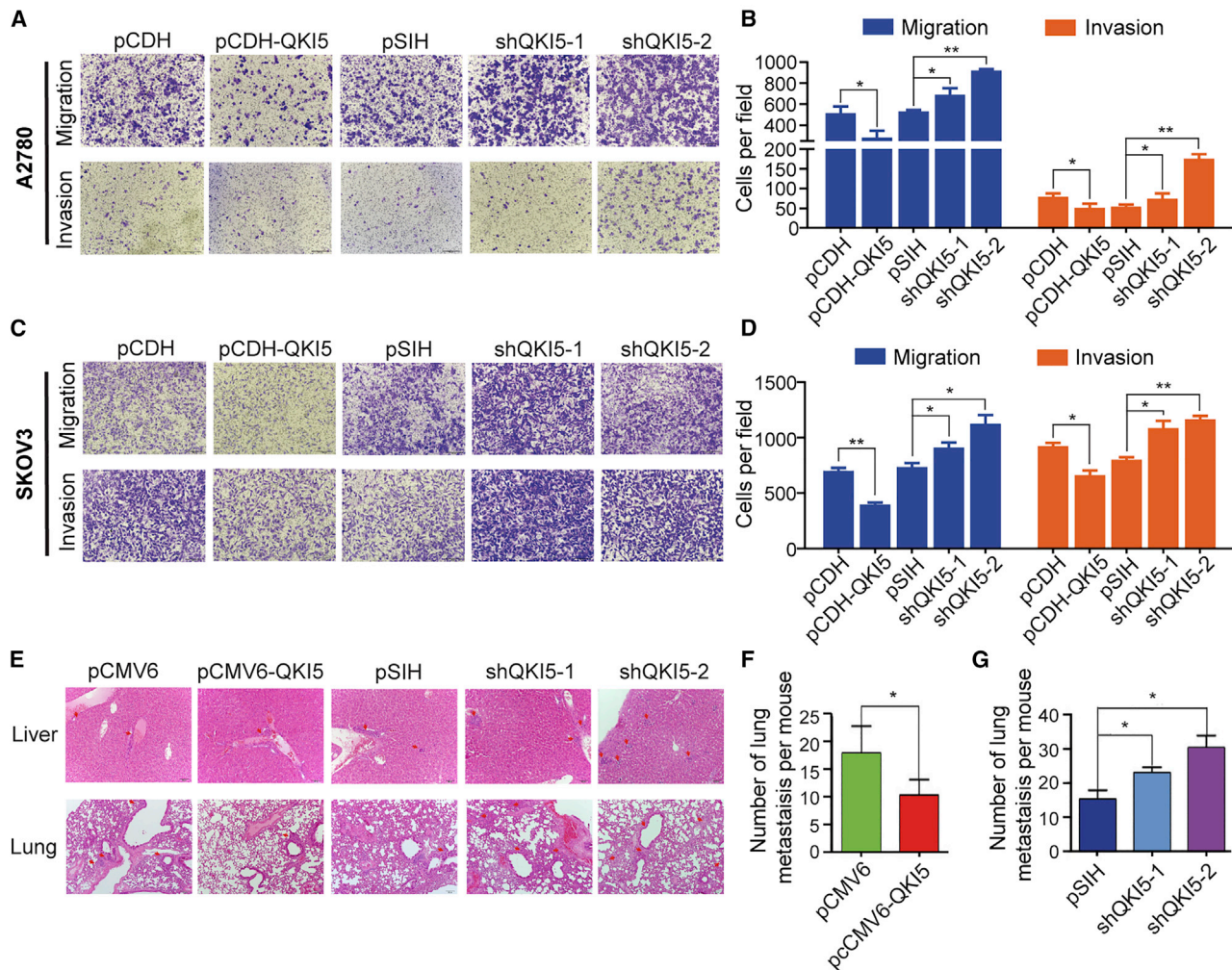


**Figure 4. QKI5 suppresses the metastasis of OC cells both *in vivo* and *in vitro***

(A–D) Transwell migration and invasion assays of A2780 and SKOV3 cells with QKI5 overexpression or knockdown. The number of migrated or invasive cells per field was calculated and shown. (E) Histological analysis of the liver and lung sections in nude mice. (F and G) The number of lung metastatic foci counted by using a microscope. Arrows indicate metastatic nodules. All data were presented as mean  $\pm$  SD. \* $p < 0.05$ , \*\* $p < 0.01$ , according to Student's *t* test.

seq) study demonstrated that QKI5 could interact with a set of genes (e.g., p27 and SOX2) involved in tumorigenesis.<sup>18,20,32</sup> However, we did not observe the alterations of these genes in our RNA-seq data. Instead, we identified TAZ and its downstream genes (CTGF and CYR61) as the targets of QKI5. This implies that QKI5 may target various genes depending on the specific cellular context.

mRNA decay is a key mode used by RBPs to control gene expression. Notably, previous genome-wide studies have demonstrated the

converse roles for QKI as the inhibitor or stabilizer of target mRNAs.<sup>17,18,33</sup> In clear cell renal cell carcinoma, QKI5 binds with Ras GTPase-activating protein 1 (RASA) mRNA to increase its stability.<sup>16</sup> On the contrary, QKI5 promotes the decay of SOX2 mRNA and FOXO1 mRNA in oral cancer cells and breast cancer cells, respectively.<sup>17,33</sup> In these cancer cells, QKI5 can act as a tumor suppressor gene by regulating the stability of different target mRNAs. Thus, transcriptome analysis of QKI5 target genes could be more comprehensive for deciphering the mechanisms of QKI5 in specific

**Figure 3. QKI5 suppresses the tumorigenesis of A2780 cells *in vivo***

(A–C) QKI5 suppressed the growth of OC xenografts. A2780 cells ( $10^6$ ) with QKI5 overexpression or silencing plasmids or empty vector were injected into the subcutaneous tissues of nude mice. Tumor size was measured every 4 days until 36 days after transplantation and the growth curves were drawn. The tumors of nude mice in each group were excised and photographed 36 days after transplantation to measure the weight of tumor. (D) Histological analysis of the tumor sections in xenotransplantation mice. Representative hematoxylin and eosin-stained images were shown and labeling with anti-Ki67 and anti-cleaved caspase-3 was performed. (E and F) The relative expression of Ki67 and cleaved caspase-3 in the tumors was shown. All data were presented as mean  $\pm$  SD. \* $p < 0.05$ , \*\* $p < 0.01$ , according to Student's *t* test.

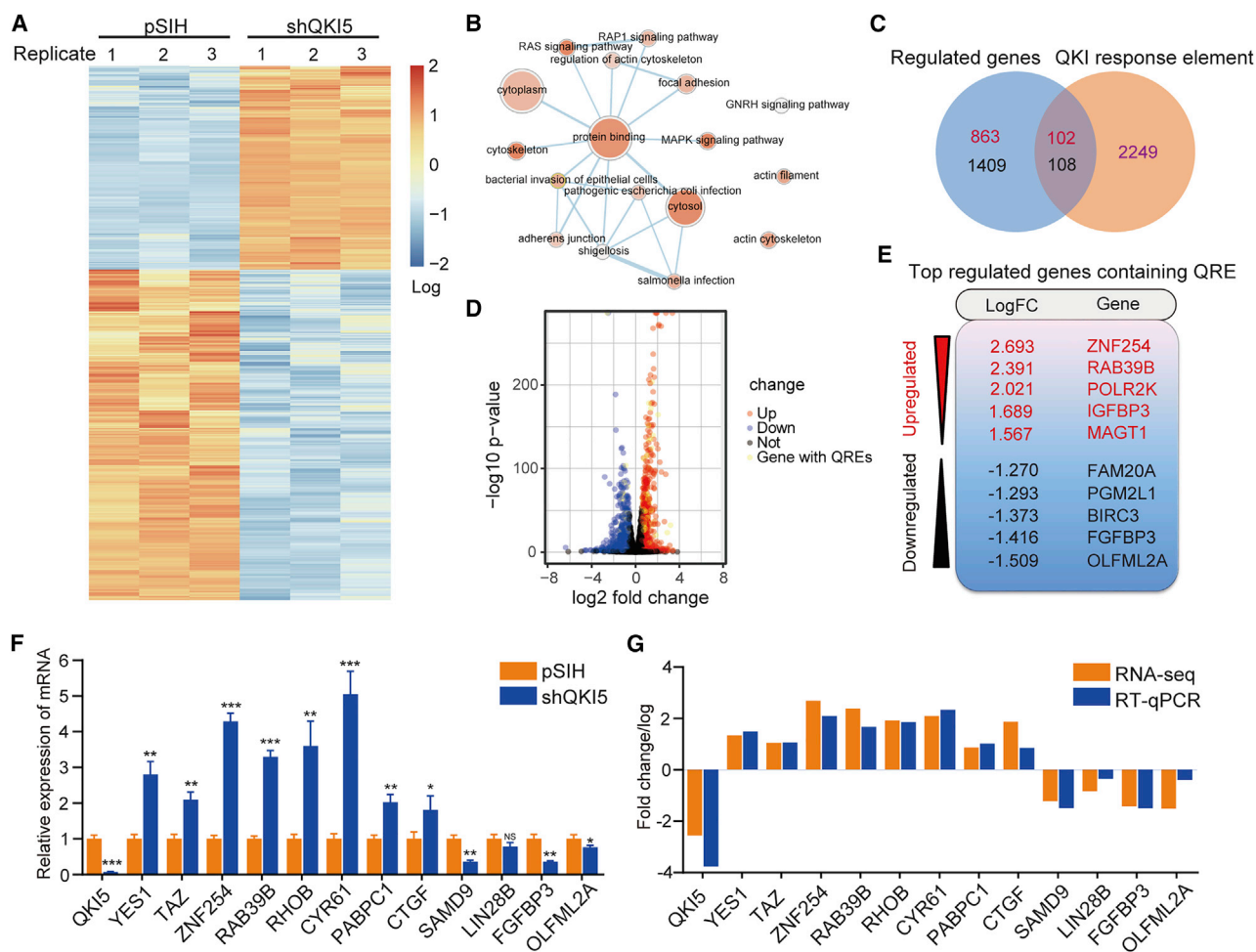


**Figure 5. QKI5 controls transcript abundance in OC cells**

(A) Heatmap shows differentially expressed genes in A2780 cells with QKI5 knockdown and control cells (fold-change > 1.5,  $p < 0.05$ ). Blue and red indicate low and high expression, respectively. (B) GO analysis of the altered genes in A2780 cells with QKI5 knockdown. (C) Venn diagrams showing differentially expressed genes and those with QRE sequences. (D) The top differentially expressed genes harboring QRE sequences were depicted. (E) Volcanic map of the transcriptome profiles between QKI5 knockdown cells and control cells. Red and blue dots indicate the significantly upregulated and downregulated genes in QKI5 knockdown cells, respectively ( $p < 0.05$ ). Orange dots represent the genes with QRE sequences. (F) qRT-PCR verified the gene alterations upon QKI5 knockdown based on the RNA-seq results (the reference gene was GAPDH). (G) A comparison between qRT-PCR results and RNA-seq data. All data were expressed as mean  $\pm$  SD. \* $p < 0.05$ , \*\* $p < 0.01$ , \*\*\* $p < 0.001$ , according to Student's t test.

cancer cells. Furthermore, the novel QKI5-TAZ regulation was identified and explored in this study. QKI5 modulates its target genes positively or negatively, but whether QKI5 can affect the overall RNA stability is awaiting further investigation.

TAZ is homologous to YES-associated protein (YAP), and both are key oncoproteins and final conduits in the Hippo pathway.<sup>34</sup> YAP and TAZ regulate the activity of transcription factors TEA domain family members (TEADs) and affect the transcription of their target genes.<sup>35</sup> The deregulation of Hippo pathway has been documented in various human carcinomas, including breast cancer, OC, and liver cancer.<sup>36–38</sup> Overexpression of TAZ in endothelial cells could induce epithelioid heman-gioendothelioma by a recurrent translocation involving TAZ-CAMTA1

fusion.<sup>39</sup> Another study showed that TAZ overexpression could predict a poor prognosis in OC patients and TAZ promoted the growth and migration of OC cells.<sup>23</sup> In our study, we found that QKI5 could negatively regulate the expression of TAZ, and the mRNA levels of these two genes were inversely correlated in OC samples, indicating that QKI5-TAZ regulation may serve as a critical factor in the progression of OC. It has been reported that TAZ promotes lung cancer cell proliferation through regulating cell cycle and apoptosis. TAZ knockdown in lung cancer cells inhibits G1/S transition and induces apoptosis.<sup>40</sup> In glioma cells, inhibition of TAZ resulted in radiation-induced senescence and growth arrest through downregulating CTGF and CYR61.<sup>41</sup> CTGF knockdown exhibits G1 arrest in follicular thyroid carcinoma cells.<sup>42</sup> CYR61 was associated with cell cycle regulation and cyclins'



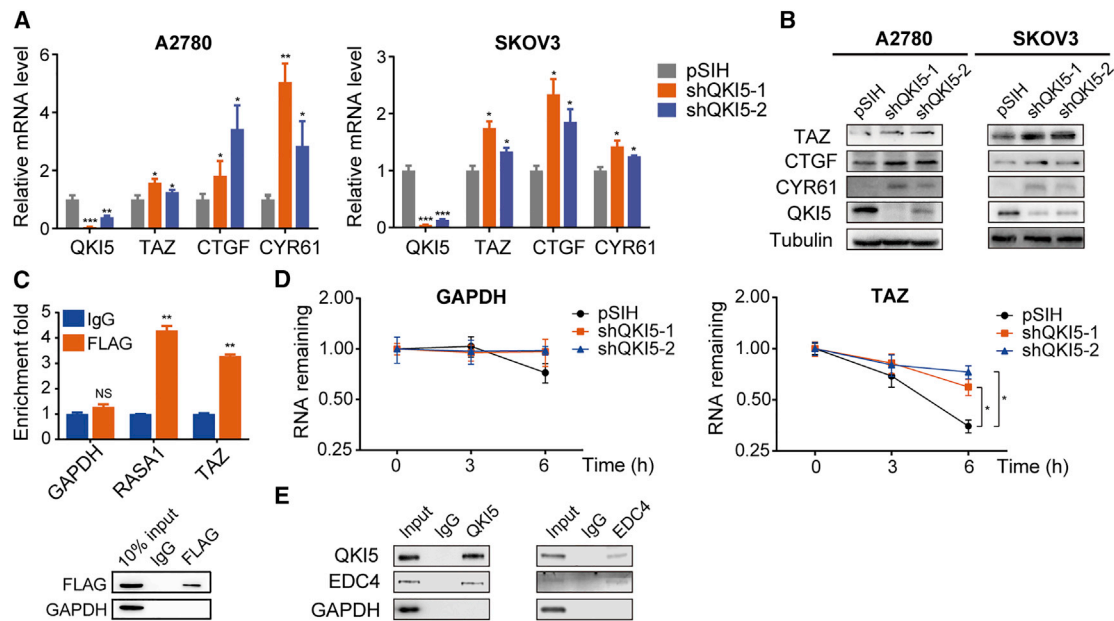


**Figure 6. QKI5 negatively regulates TAZ expression in OC cells**

(A) The expression levels of QKI5, TAZ, CTGF, and CYR61 in OC cells with QKI5 knockdown were detected by qRT-PCR (GAPDH was used as the reference gene). (B) The protein levels of QKI5, TAZ, CTGF, and CYR61 in OC cells after QKI5 knockdown were detected by immunoblotting (tubulin was used as the reference gene). (C) qRT-PCR and immunoblotting analyses were conducted to determine RIP-derived RNA and protein, respectively. The enrichment fold of qRT-PCR products was expressed normalized to IgG. GAPDH was employed as the negative control in qRT-PCR and immunoblotting assays; while RASA1 was employed as the positive control in qRT-PCR assays. (D) qRT-PCR was used to assess the stability of TAZ and GAPDH mRNA in A2780 cells with QKI5 knockdown and control cells over time after treatment with 50  $\mu$ M actinomycin D, and then normalized to 18S rRNA. (E) The interaction between QKI5 and EDC4 was evaluated by IP and immunoblotting. All data were presented as mean  $\pm$  SD. NS, not significant, \* $p < 0.05$ , \*\* $p < 0.01$ , \*\*\* $p < 0.001$ , according to Student's *t* test.

expression in progressive mantle cell lymphoma.<sup>43</sup> These studies suggest that TAZ-CTGF/CYR61 regulation could affect the cell cycle and apoptosis. Alternatively, we could not exclude that QKI5 might affect the cell cycle and apoptosis through other factors involved in cell cycle and apoptosis regulation as QKI5 could regulate expression of multiple genes. Despite this, our study proposed that QKI5 might regulate the cell cycle and apoptosis through TAZ-CTGF/CYR61 regulation. Collectively, our findings provide strong evidence that TAZ is involved in the QKI5-mediated tumor suppression of OC cells and reveal a novel QKI5-TAZ regulation in OC patients, which may help to illuminate the underlying pathogenetic mechanisms and develop a better treatment.

## MATERIALS AND METHODS

### Tumor tissues

hNOSE samples were collected from the ovaries of donors. Frozen specimens and formalin-fixed paraffin-embedded (FFPE) samples of hNOSE and SOC were collected from Daping hospital. All OC tissues and tissue microarrays were reviewed by the pathologist, and the information of patients was described in our previous study.<sup>15</sup>

### Plasmid construction

QKI5 cDNA was synthesized by RT-PCR and then cloned into pCDH or pCMV6 vectors. For short hairpin RNA (shRNA) construction, both sense and antisense (reverse complement) oligonucleotides

targeting QKI5 or TAZ were annealed and inserted into the pSIH or pLKO.1 vectors.

### Cell culture

HEK293T cell line was maintained in DMEM (GIBCO) containing 10% fetal bovine serum (FBS, AusGeneX) and 1% streptomycin/penicillin (GIBCO) at 37°C and 5% CO<sub>2</sub>. A2780 and SKOV3 OC cell lines were cultured in RPMI-1640 (GIBCO) with 10% FBS and 1% streptomycin/penicillin (GIBCO). Where indicated, A2780 cell line was treated with actinomycin D (Solarbio) at the indicated times prior to RNA stability assay.

### Cell viability

The cells were grown in 96-well plates, pretreated at 0, 24, 48, 72, and 96 h, and then exposed to CCK-8 (DOJINDO) for 2 h. The absorbance was read at 450 nm using a microplate reader.

### Apoptosis and cell cycle assays

Regarding apoptosis analysis, the cell lines were pretreated with H<sub>2</sub>O<sub>2</sub> for 4 h, stained by Annexin V Apoptosis Detection Kit (DOJINDO), and then assessed using an Accuri C6 flow cytometer (BD Biosciences). As for cell cycle assessment, the cell lines were fixed, treated with RNase (Invitrogen), stained by propidium iodide (PI, Invitrogen), and then examined using the Accuri C6 flow cytometer (BD Biosciences).

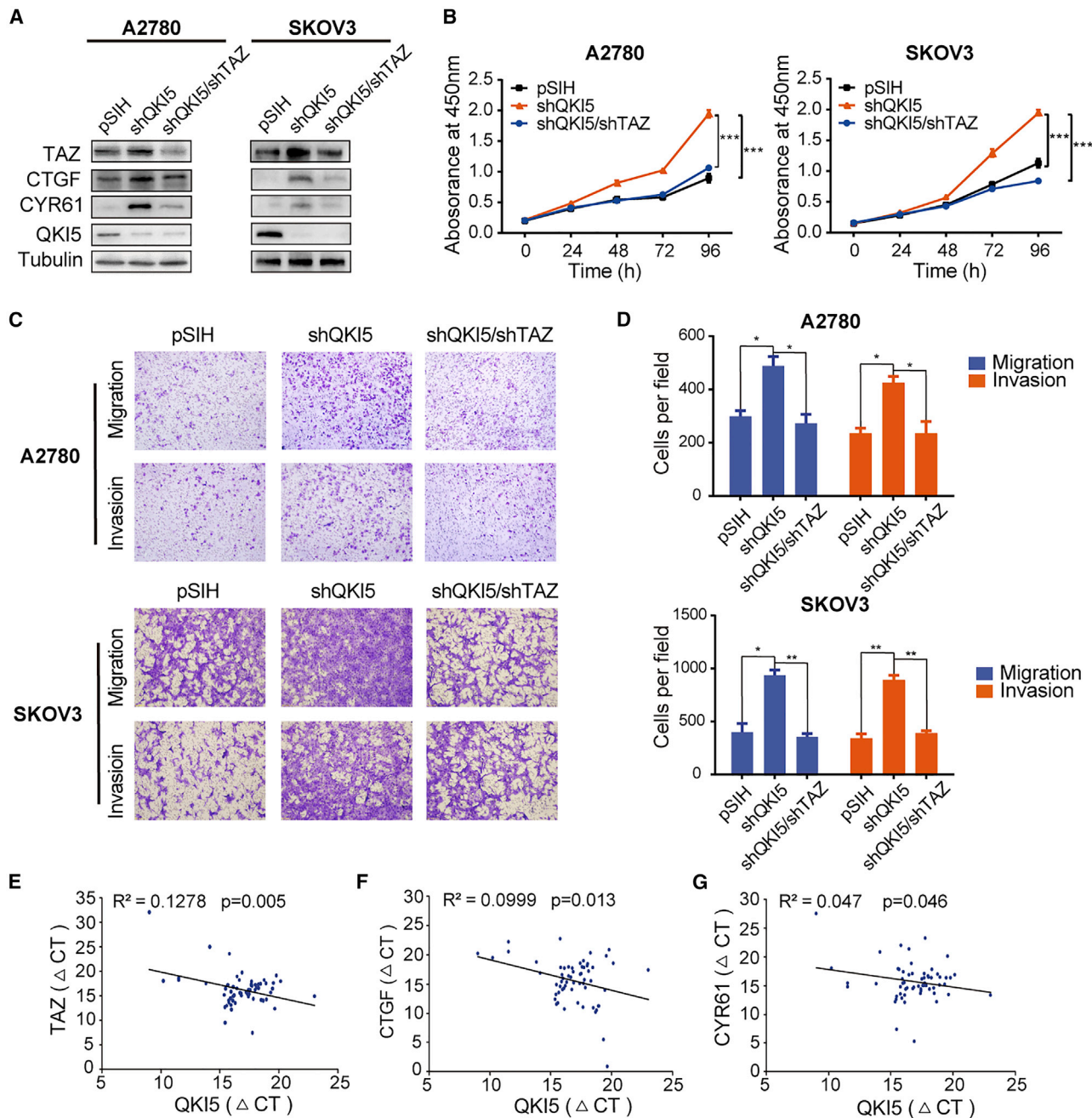


**Figure 7. TAZ is involved in the QKI5-mediated tumor suppression of OC**

(A) The protein levels of QKI5, TAZ, CTGF, and CYR61 in OC cells after QKI5 and TAZ knockdown were detected by immunoblotting (tubulin was used as the reference gene). (B) Effect of QKI5 knockdown with/without TAZ knockdown on OC cell growth, as revealed by CCK-8 assays. (C and D) The migration and invasion abilities of A2780 and SKOV3 cells after QKI5 knockdown with/without TAZ knockdown. The number of migrated or invasive cells per field was calculated and shown. (E–G) The correlation of QKI5 expression with TAZ, CTGF, and CYR61 expression was determined in a set of OC tissues (n = 41) and normal ovarian epithelial tissues (n = 19). Pearson correlation analysis was performed for  $\Delta$ CT values (after normalization to 18S rRNA). All data were expressed as mean  $\pm$  SD. \* $p < 0.05$ , \*\* $p < 0.01$ , \*\*\* $p < 0.001$ , according to Student's t test.

**Immunohistochemistry**

Immunohistochemistry was performed as described in the previous study. Briefly, FFPE samples were dewaxed and soaked with peroxidase-3%  $H_2O_2$ . Then, sodium citrate (10 mM, pH 6.0) was

utilized for the antigen retrieval. After blocking with 5% BSA in PBS, the samples were incubated with anti-QKI5 (1:1,000, Millipore) antibody at 4°C overnight. A composite score was evaluated according to the standard formula described in our previous study.<sup>15</sup>

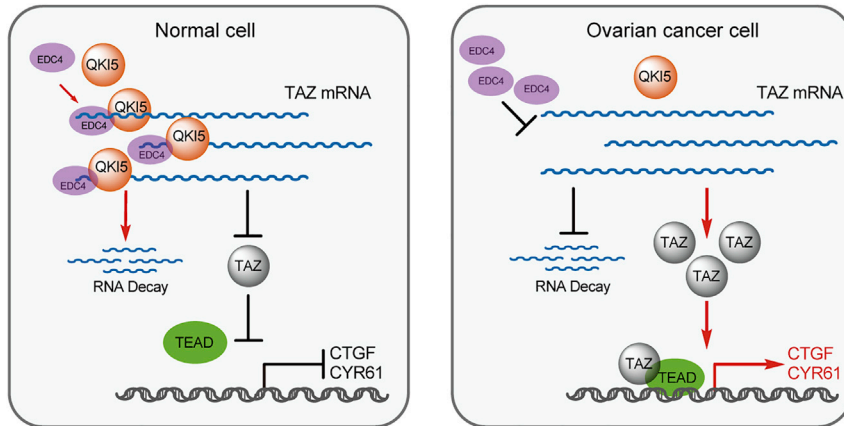


**Figure 8. Proposed model of QKI5 downregulating the expression of TAZ in OC**

For RNA-seq, NEBNext poly(A) mRNA Magnetic Isolation Module was employed to purify the poly(A) mRNA. Then, library preparation was conducted using a NEBNext Ultra Directional RNA Library Prep Kit (New England BioLabs, Ipswich, MA, USA). Illumina HiSeq 1000 with paired-end 150-bp read length was used for sequencing. mRNA clean reads were mapped to UCSC hg38 primary assembly genome using TopHat2 software. HTSeq was used to calculate counts among transcripts. Bioconductor package DESeq2 was used for read

normalization, size factor estimation, and differential expression analysis, and then bioinformatics analysis was conducted in R expression quantification.

#### Co-IP and mass spectrometry

Cells were pelleted, rinsed, and then lysed in IP lysis buffer (20% glycerol, 0.2 mM EDTA, 50 mM KCl, 50 mM Tris, and 150 mM NaCl) containing protease inhibitor cocktail and 0.1% NP40 (Solarbio). Following the addition of antibodies, the lysates were incubated with protein G beads (50  $\mu$ L, Invitrogen) for 4 h at 4°C. After rinsing, the proteins were collected, fractionated through SDS-PAGE, and measured by immunoblotting. For mass spectrum, the co-precipitated proteins were analyzed by silver staining and then subjected to mass spectrometry analysis.

#### RIP

The cells were pelleted and then lysed in IP lysis buffer with RNase inhibitor (Thermo Fisher Scientific). The lysates with 3  $\mu$ g antibody were incubated with protein G beads (50  $\mu$ L, Invitrogen) for 4 h at 4°C. After rinsing, the co-precipitated RNA was extracted by TRI Reagent, treated with DNase, and then detected by qRT-PCR.

#### Statistical tests

The specific statistical test used is described in each figure legend, together with the significant p values. SPSS 16.0 was used for performing both survival and immunohistochemical analyses, while other tests were conducted using GraphPad Prism 6.0. The significance threshold was set at  $p < 0.05$ .

#### SUPPLEMENTAL INFORMATION

Supplemental information can be found online at <https://doi.org/10.1016/j.omtn.2021.07.012>.

#### ACKNOWLEDGMENTS

This work was sponsored by the National Natural Science Foundation of China (81902668), the Natural Science Foundation of Chongqing,

#### Immunoblotting

The cell lines were rinsed in PBS, pelleted, and then incubated with lysis buffer on ice for 30 min. After centrifugation (16,000  $\times$  g, 10 min, 4°C), the lysate was harvested, separated by SDS-PAGE, and then blotted. The following antibodies were used: anti-QKI5 (1:2,000, Millipore), anti-tubulin (1:10,000), anti-GAPDH (1:5,000), anti-TAZ (1:500), anti-CTGF (1:50), anti-CYR61 (1:500), and anti-EDC4 (1:1,000). All these antibodies were obtained from Proteintech (USA), unless otherwise specified.

#### Cell migration and invasion assays

Cell migration assay was carried out through the Transwell chamber system (Corning). Briefly,  $10^4$  cells were added in the top chamber containing serum-free culture medium, while the bottom chamber filled with the culture medium containing 20% FBS. After 24 h, the cells were fixed and then stained with crystal violet. For cell invasion assay, Matrigel (Corning) was added to the upper chamber before plating cells. All experiments were performed independently three times.

#### Animal assays

For tumorigenesis assay, cells ( $5 \times 10^6$ ) were subcutaneously injected into BALB/C nude mice. The volume and weight of tumors were measured every 4 days for 36 days. For cell metastasis assay,  $1 \times 10^6$  cells were injected into the lateral tail vein of mice. After 5 weeks of injection, all mice were executed. The lungs and livers were isolated, fixed, paraffin embedded, and then stained with hematoxylin and eosin. The animal experiments were approved by the Institutional Animal Care and Use Committee of Daping Hospital and the care was in accordance with institution guidelines.

#### RNA isolation, qRT-PCR, and RNA-seq

TRI Reagent (Sigma-Aldrich) was used to extract total RNA in compliance with the reagent protocol. qRT-PCR was conducted to measure the RNA level using a QuantStudio 5 Dx Real-Time PCR System (Applied Biosystems, Life Technologies). The oligonucleotides used for qRT-PCR are presented in Table S3.



China (csc2020jcyj-msxmX0344), the Social Undertakings and People's Livelihood Security Innovation of Science and Technology Special Project of Chongqing Yubei District Science and Technology Bureau, China (KY19036), China Postdoctoral Science Foundation (2021M693927), and the Incubation Program of the Third Affiliated Hospital of Chongqing Medical University, China (KY08027). The authors would like to express their gratitude to EditSprings for the expert linguistic services provided.

#### AUTHOR CONTRIBUTIONS

P.Y. and Jia Yu supervised the project; T.L., Y.Y., Z.X., D.Y., X.L., H.Z., Q.W., Y.L., and L.L. performed the experiments; Jianhua Yu, Y.W., F.W., and J.X. helped analyze the data; T.L. and P.Y. wrote and reviewed the manuscript.

#### DECLARATION OF INTERESTS

The authors declare no competing interests.

#### REFERENCES

- Siegel, R.L., Miller, K.D., and Jemal, A. (2019). Cancer statistics, 2019. *CA Cancer J. Clin.* *69*, 7–34.
- Karnezis, A.N., Cho, K.R., Gilks, C.B., Pearce, C.L., and Huntsman, D.G. (2017). The disparate origins of ovarian cancers: pathogenesis and prevention strategies. *Nat. Rev. Cancer* *17*, 65–74.
- Peres, L.C., Cushing-Haugen, K.L., Köbel, M., Harris, H.R., Berchuck, A., Rossing, M.A., Schildkraut, J.M., and Doherty, J.A. (2019). Invasive Epithelial Ovarian Cancer Survival by Histotype and Disease Stage. *J. Natl. Cancer Inst.* *111*, 60–68.
- Mabuchi, S., Kuroda, H., Takahashi, R., and Sasano, T. (2015). The PI3K/AKT/mTOR pathway as a therapeutic target in ovarian cancer. *Gynecol. Oncol.* *137*, 173–179.
- Hsu, C.Y., Bristow, R., Cha, M.S., Wang, B.G., Ho, C.L., Kurman, R.J., Wang, T.L., and Shih I, M. (2004). Characterization of active mitogen-activated protein kinase in ovarian serous carcinomas. *Clin Cancer Res* *10*, 6432–6436.
- Xu, F., Yu, Y., Le, X.F., Boyer, C., Mills, G.B., and Bast, R.C., Jr. (1999). The outcome of heregulin-induced activation of ovarian cancer cells depends on the relative levels of HER-2 and HER-3 expression. *Clin Cancer Res* *5*, 3653–3660.
- Gerstberger, S., Hafner, M., and Tuschl, T. (2014). A census of human RNA-binding proteins. *Nat. Rev. Genet.* *15*, 829–845.
- Beckmann, B.M., Horos, R., Fischer, B., Castello, A., Eichelbaum, K., Alleaume, A.M., Schwarzl, T., Curk, T., Foehr, S., Huber, W., et al. (2015). The RNA-binding proteomes from yeast to man harbour conserved enigmRBPs. *Nat. Commun.* *6*, 10127.
- Tan, Q., Yalamanchili, H.K., Park, J., De Maio, A., Lu, H.C., Wan, Y.W., White, J.J., Bondar, V.V., Sayegh, L.S., Liu, X., et al. (2016). Extensive cryptic splicing upon loss of RBM17 and TDP43 in neurodegeneration models. *Hum. Mol. Genet.* *25*, 5083–5093.
- Wang, Z.L., Li, B., Luo, Y.X., Lin, Q., Liu, S.R., Zhang, X.Q., Zhou, H., Yang, J.H., and Qu, L.H. (2018). Comprehensive Genomic Characterization of RNA-Binding Proteins across Human Cancers. *Cell Rep.* *22*, 286–298.
- Wang, F., Song, W., Zhao, H., Ma, Y., Li, Y., Zhai, D., Pi, J., Si, Y., Xu, J., Dong, L., et al. (2017). The RNA-binding protein QKI5 regulates primary miR-124-1 processing via a distal RNA motif during erythropoiesis. *Cell Res.* *27*, 416–439.
- Hayakawa-Yano, Y., Suyama, S., Nogami, M., Yugami, M., Koya, I., Furukawa, T., Zhou, L., Abe, M., Sakimura, K., Takebayashi, H., et al. (2017). An RNA-binding protein, Qki5, regulates embryonic neural stem cells through pre-mRNA processing in cell adhesion signaling. *Genes Dev.* *31*, 1910–1925.
- Novikov, L., Park, J.W., Chen, H., Klerman, H., Jalloh, A.S., and Gamble, M.J. (2011). QKI-mediated alternative splicing of the histone variant MacroH2A1 regulates cancer cell proliferation. *Mol. Cell. Biol.* *31*, 4244–4255.
- Zong, F.Y., Fu, X., Wei, W.J., Luo, Y.G., Heiner, M., Cao, L.J., Fang, Z., Fang, R., Lu, D., Ji, H., and Hui, J. (2014). The RNA-binding protein QKI suppresses cancer-associated aberrant splicing. *PLoS Genet.* *10*, e1004289.
- Li, L., Luo, Q., Xie, Z., Li, G., Mao, C., Liu, Y., Wen, X., Yin, N., Cao, J., Wang, J., et al. (2016). Characterization of the Expression of the RNA Binding Protein eIF4G1 and Its Clinicopathological Correlation with Serous Ovarian Cancer. *PLoS ONE* *11*, e0163447.
- de Bruin, R.G., Shiue, L., Prins, J., de Boer, H.C., Singh, A., Fagg, W.S., van Gils, J.M., Duijjs, J.M., Katzman, S., Kraaijeveld, A.O., et al. (2016). Quaking promotes monocyte differentiation into pro-atherogenic macrophages by controlling pre-mRNA splicing and gene expression. *Nat. Commun.* *7*, 10846.
- Zhang, R.-L., Yang, J.-P., Peng, L.-X., Zheng, L.-S., Xie, P., Wang, M.-Y., Cao, Y., Zhang, Z.-L., Zhou, F.-J., Qian, C.-N., and Bao, Y.X. (2016). RNA-binding protein QKI-5 inhibits the proliferation of clear cell renal cell carcinoma via post-transcriptional stabilization of RASA1 mRNA. *Cell Cycle* *15*, 3094–3104.
- Lu, W., Feng, F., Xu, J., Lu, X., Wang, S., Wang, L., Lu, H., Wei, M., Yang, G., Wang, L., et al. (2014). QKI impairs self-renewal and tumorigenicity of oral cancer cells via repression of SOX2. *Cancer Biol. Ther.* *15*, 1174–1184.
- de Miguel, F.J., Pajares, M.J., Martínez-Terroba, E., Ajona, D., Morales, X., Sharma, R.D., Pardo, F.J., Rouzaut, A., Rubio, A., Montuenga, L.M., and Pio, R. (2016). A large-scale analysis of alternative splicing reveals a key role of QKI in lung cancer. *Mol. Oncol.* *10*, 1437–1449.
- Galarnau, A., and Richard, S. (2005). Target RNA motif and target mRNAs of the Quaking STAR protein. *Nat. Struct. Mol. Biol.* *12*, 691–698.
- Lai, D., Ho, K.C., Hao, Y., and Yang, X. (2011). Taxol resistance in breast cancer cells is mediated by the hippo pathway component TAZ and its downstream transcriptional targets Cyr61 and CTGF. *Cancer Res.* *71*, 2728–2738.
- Zhang, H., Liu, C.Y., Zha, Z.Y., Zhao, B., Yao, J., Zhao, S., Xiong, Y., Lei, Q.Y., and Guan, K.L. (2009). TEAD transcription factors mediate the function of TAZ in cell growth and epithelial-mesenchymal transition. *J. Biol. Chem.* *284*, 13355–13362.
- Chen, G., Xie, J., Huang, P., and Yang, Z. (2016). Overexpression of TAZ promotes cell proliferation, migration and epithelial-mesenchymal transition in ovarian cancer. *Oncol. Lett.* *12*, 1821–1825.
- Chang, C.T., Muthukumar, S., Weber, R., Levinsky, Y., Chen, Y., Bhandari, D., Igreja, C., Wohlbold, L., Valkov, E., and Izaurralde, E. (2019). A low-complexity region in human XRN1 directly recruits deadenylation and decapping factors in 5'-3' messenger RNA decay. *Nucleic Acids Res.* *47*, 9282–9295.
- Wu, J., Zhou, L., Tonissen, K., Tee, R., and Artzt, K. (1999). The quaking 1-5 protein (QKI-5) has a novel nuclear localization signal and shuttles between the nucleus and the cytoplasm. *J. Biol. Chem.* *274*, 29202–29210.
- Hardy, R.J., Loushin, C.L., Friedrich, V.L., Jr., Chen, Q., Ebersole, T.A., Lazzarini, R.A., and Artzt, K. (1996). Neural cell type-specific expression of QKI proteins is altered in quakingviable mutant mice. *J. Neurosci.* *16*, 7941–7949.
- Vernet, C., and Artzt, K. (1997). STAR, a gene family involved in signal transduction and activation of RNA. *Trends Genet.* *13*, 479–484.
- Ebersole, T.A., Chen, Q., Justice, M.J., and Artzt, K. (1996). The quaking gene product necessary in embryogenesis and myelination combines features of RNA binding and signal transduction proteins. *Nat. Genet.* *12*, 260–265.
- Kondo, T., Furuta, T., Mitsunaga, K., Ebersole, T.A., Shichiri, M., Wu, J., Artzt, K., Yamamura, K., and Abe, K. (1999). Genomic organization and expression analysis of the mouse qki locus. *Mammalian genome* *10*, 662–669.
- Chen, Y., Tian, D., Ku, L., Osterhout, D.J., and Feng, Y. (2007). The selective RNA-binding protein quaking I (QKI) is necessary and sufficient for promoting oligodendroglia differentiation. *J. Biol. Chem.* *282*, 23553–23560.
- Larocque, D., and Richard, S. (2005). QUAKING KH domain proteins as regulators of glial cell fate and myelination. *RNA Biol.* *2*, 37–40.
- Hafner, M., Landthaler, M., Burger, L., Khorshid, M., Hausser, J., Berninger, P., Rothballer, A., Ascano, M., Jr., Jungkamp, A.C., Munschauer, M., et al. (2010). Transcriptome-wide identification of RNA-binding protein and microRNA target sites by PAR-CLIP. *Cell* *141*, 129–141.

33. Yu, F., Jin, L., Yang, G., Ji, L., Wang, F., and Lu, Z. (2014). Post-transcriptional repression of FOXO1 by QKI results in low levels of FOXO1 expression in breast cancer cells. *Oncol. Rep.* *31*, 1459–1465.
34. Huang, J., Wu, S., Barrera, J., Matthews, K., and Pan, D. (2005). The Hippo signaling pathway coordinately regulates cell proliferation and apoptosis by inactivating Yorkie, the *Drosophila* Homolog of YAP. *Cell* *122*, 421–434.
35. Hong, W., and Guan, K.L. (2012). The YAP and TAZ transcription co-activators: key downstream effectors of the mammalian Hippo pathway. *Semin. Cell Dev. Biol.* *23*, 785–793.
36. Lu, L., Li, Y., Kim, S.M., Bossuyt, W., Liu, P., Qiu, Q., Wang, Y., Halder, G., Finegold, M.J., Lee, J.S., and Johnson, R.L. (2010). Hippo signaling is a potent *in vivo* growth and tumor suppressor pathway in the mammalian liver. *Proc. Natl. Acad. Sci. USA* *107*, 1437–1442.
37. Li, H., Wang, S., Wang, G., Zhang, Z., Wu, X., Zhang, T., Fu, B., and Chen, G. (2014). Yes-associated protein expression is a predictive marker for recurrence of hepatocellular carcinoma after liver transplantation. *Dig. Surg.* *31*, 468–478.
38. Zhang, X., George, J., Deb, S., Degoutin, J.L., Takano, E.A., Fox, S.B., Bowtell, D.D., and Harvey, K.F.; AOCs Study group (2011). The Hippo pathway transcriptional co-activator, YAP, is an ovarian cancer oncogene. *Oncogene* *30*, 2810–2822.
39. Tanas, M.R., Ma, S., Jadaan, F.O., Ng, C.K., Weigelt, B., Reis-Filho, J.S., and Rubin, B.P. (2016). Mechanism of action of a WWTR1(TAZ)-CAMTA1 fusion oncoprotein. *Oncogene* *35*, 929–938.
40. Noguchi, S., Saito, A., Horie, M., Mikami, Y., Suzuki, H.I., Morishita, Y., Ohshima, M., Abiko, Y., Mattsson, J.S., Konig, H., et al. (2014). An integrative analysis of the tumorigenic role of TAZ in human non-small cell lung cancer. *Clin Cancer Res* *20*, 4660–4672.
41. Zhang, L., Cheng, F., Wei, Y., Zhang, L., Guo, D., Wang, B., and Li, W. (2019). Inhibition of TAZ contributes radiation-induced senescence and growth arrest in glioma cells. *Oncogene* *38*, 2788–2799.
42. Sun, D., Han, S., Liu, C., Zhou, R., Sun, W., Zhang, Z., and Qu, J. (2016). MicroRNA-199a-5p Functions as a Tumor Suppressor via Suppressing Connective Tissue Growth Factor (CTGF) in Follicular Thyroid Carcinoma. *Med. Sci. Monit.* *22*, 1210–1217.
43. Zaidi, A.R.S., Dresman, S., Burt, C., Rule, S., and McCallum, L. (2019). Molecular signatures for CCN1, p21 and p27 in progressive mantle cell lymphoma. *J. Cell Commun. Signal.* *13*, 421–434.